PCCP

Adsorption and Splitting of H2S on 2D-ZnO_1-xN_y: First-principle Analysis

Journal:	*Physical Chemistry Chemical Physics*
Manuscript ID:	CP-ART-03-2014-001092
Article Type:	Paper
Date Submitted by the Author:	13-Mar-2014

Complete List of Authors:	Kouser, Summayya; JNCASR, TSU Waghmare, Umesh V; Jawaharlal Nehru Centre for Advanced Scientific Research, Theoretical Sciences Unit Tit, Nacir; UAE University, Physics

Physical Chemistry Chemical Physics
CREATED USING THE RSC LaTeX PCCP ARTICLE TEMPLATE – SEE www.rsc.org/electronicfiles FOR DETAILS
ARTICLE TYPE www. rsc.org/xxxxxx | XXXXXXXX

Adsorption and Splitting of H_2S on 2D-$ZnO_{1-x}N_y$: First-principles Analysis

Summayya Kouser,[a] Umesh V. Waghmare,[a,b‡] and Nacir Tit[c*]

Received Xth XXXXXXXXXX 20XX, Accepted Xth XXXXXXXXX 20XX
First published on the web Xth XXXXXXXXXX 200X
DOI: 10.1039/b000000x

We present a thorough analysis of molecular adsorption of a toxic gas, H_2S, on pristine, defective and N-substituted 2D-ZnO using first-principles simulations within density functional theory and parametrized form of van der Waals (vdW) interaction. We find that the binding of H_2S with pristine 2D-ZnO is relatively weak (adsorption energy $E_A = -29$ to -36 kJmol^{-1}) as it is mainly through vdW interaction. However, substitutional nitrogen doping in 2D-ZnO leads to a drastic increase in the adsorption energy ($E_A = -152$ kJmol^{-1}) resulting in dissociation of H_2S molecule. This originates fundamentally from a strong covalent bonding interaction between an unpaired electron in the p-orbital of nitrogen with electron in s-orbital of H. While O-vacancy in 2D-ZnO has little effect on its interaction with H_2S at lower coverages, a strong interaction at higher coverages leads to splitting of H_2S and formation of H_2 molecule. Our work shows that 2D-ZnO is a promising material to facilitate capturing of toxic H_2S from environment and at the same time converting it to a green source of energy.

1 Introduction

Hydrogen sulphide is a toxic and corrosive gas; exposure to H_2S causes broad range of health problems at low concentrations and can be lethal when inhaled in large concentrations.[1] H_2S is released in significant quantities in many industrial processes which include natural gas processing, petroleum refining, mining, and paper and pulp processing. Many methods have been implemented for the removal of H_2S in environment such as biological fixation, iron chloride dosing, water scrubbing etc.[2] These methods are either expensive or demanding in terms of their foot-print.

Dissociation of H_2S leading to non-toxic by-products is one of the possible solutions.[3,4] The Claus process is widely used for dissociation of H_2S in industries, but the main drawback is that the by-product is (H_2O) instead of clean fuel (H_2).[5] Thermal decomposition of H_2S into H_2 and S has been investigated and is thermodynamically unfavorable.[6] Here, we explore the possibility of using a nano-material to facilitate splitting H_2S into H_2 and atomic S through chemical interaction, with two-fold goals: (i) elimination of toxic gas from environment, and (ii) production of clean energy fuel (H_2) with much lower heat of formation (-4.77 kcal mol^{-1}) than H_2O (-68.32 kcal mol^{-1}). Needless to say, another application of the same material would be in the gas sensing.

Semiconducting metal oxides (SMO) nanoparticles have been natural candidates for gas sensing applications due to (i) large surface-to-volume ratio, (ii) high sensitivity to gaseous exposure through change in their conductivities due to surface electron accumulation,[7,8] and (iii) a low fabrication cost. Gas sensing is essential for industrial process control, safety systems and environmental monitoring.[9,10] Many semiconducting metal oxides are known for their use as gas sensors. For instance, Comini *et al*,[11] have used SnO_2 nanobelts for the effective detection of pollutants like CO and NO_2 and C_2H_5OH in breath analyzers and food control applications. Chao *et al*,[12] have used In_2O_3 nanowires for detection of small amounts of NO_2 and NH_3, and showed (a) a significant change in conductance (as high as 10^5 to 10^6 times), and (b) very short recovery time of the device by illuminating with UV light. Other metal oxides such as TiO_2, ZnO and Fe_2O_3 are also known for applications as gas sensors.[12–14]

Change in conductivity resulting from the interaction with a gas necessarily involves modification of the electronic structure and bonding. Hence, SMO (eg. TiO_2, Fe_2O_3) have also been known for hydrogen fuel production by dissociation of H_2O.[15,16] Since the O and S belong to same group, we expect SMO to possibly facilitate the process of dissociation of H_2S. Rate of reaction of H_2S with different metal oxides surfaces such as Cr_2O_3, Al_2O_3 and ZnO have been studied and known to be inversely proportional to band gap of the metal oxide.[4,17] To this end, N-substitution in ZnO is known to reduce its gap, and can be effective in enhancing its interaction with H_2S.[18]

In the bulk form, ZnO is a wide band-gap semiconductor (3.37 eV) with high exciton binding energy (60 meV) and a large piezoelectric constant.[19–22] The band gap of ZnO can be engineered by alloying with MgO and CdO, which is useful for optoelectronic devices.[23–25] Its unique set of properties make it useful in many applications such as transparent electronics, spintronics, piezoelectric devices, optical devices and

chemical sensors. Central to these is its ability to exist in diverse forms of nanostructures, which makes it a key technological material. Theoretical prediction of 2D-ZnO (inorganic analogue of graphene) with large surface area and a wide band gap ($E^{GW} = 3.57eV$)[26] make it an interesting candidate for gas adsorption/dissociation.

In addition to temperature, size and dimensionality, the presence of native defects and doping with impurities or promoters also influence the rate of adsorption and dissociation. Ahn *et al*,[27] have shown that gas sensing behaviour is linearly proportional to the photoluminescence intensity of oxygen vacancies. Zhang and coworkers,[28] have reported that doping graphene with transition metal atoms like Ca, Co, Fe or Si lead to chemisorption of H_2S as compared to its weaker physisortion on pristine graphene. Lee and coworkers,[29] have shown 100% recovery and drastic improvement to the sensing ability of SnO_2 in detecting very low concentrations of H_2S (< 1 ppm) using MoO_3 and NiO as promoters. Bikondoa *et al*,[16] have shown defect (O-vacancy) mediated splitting of H_2O in thin-film of TiO_2. However, Hegde *et al*,[30] have studied adsorption of H_2S on pristine graphene and graphene with defects, and showed that H_2S interacts weakly through vdW interaction with both pristine graphene and graphene with defects.[30]

In this article, we have studied the adsorption and possible modes of dissociation of H_2S gas on pristine 2D-ZnO, and explored how it can be enhanced through (a) substitutional nitrogen doping at oxygen sites and (b) introduction of O-vacancy. We have also examined the possiblity of existence of Stone-Wales in 2D-ZnO, that might alter its interaction with H_2S. In section II, we describe computational details, and present extensive results for the adsorptive interaction between H_2S and 2D-ZnO as a function of coverage and concentration of defect or impurities in section III. This is followed by conclusions in section IV, highlighting the relevance of our work to applications in environment and energy.

2 Computational Methods

Our first-principles calculations are based on density functional theory (DFT) as implemented in QUANTUM ESPRESSO package.[31] A local density approximation to the exchange correlation energy functional is known to overestimate the binding energies, particularly the interaction of molecules with a surface. We have used a generalized gradient approximation (GGA) of Perdew Burke-Ernzehof (PBE) parameterized form[32] because the charge density varies more rapidly in the space between a molecule and the adsorbing surface, and gradient corrections can be significant. Secondly, such interaction involves van der Waals (vdW) long range interactions whose parameterization is available along with a GGA functional implemented using Grimme scheme.[33] Since the improvised GGA functionals are known to give more accurate binding energies,[34–36] we adopt the use of GGA in present calculations. We use plane wave basis with energy cutoffs of 30 Ry and of 180 Ry in representation of wave function and density respectively, and ultrasoft pseudopotentials[37] to represent the interaction between ionic cores and valence electrons. We employ periodic boundary conditions with 3 x 3 x 1 or 4 x 4 x 1 supercell (18 or 32 atoms) of 2D-ZnO with different concentrations of coverage of H_2S, and include a vaccum of 12 Å, in the direction perpendicular to 2D-ZnO sheet to keep interactions between periodic images low. We use uniform mesh of 7 x 7 x 1 k-points in sampling integrations over Brilloiun zone, and smear the occupation numbers of electronic states with Fermi-Dirac distribution and smearing width (k_BT) of 0.04 eV. We consider configurations with different structural orientations and coverage of H_2S varying defect concentration and relax the structure to minimize energy until the Hellmann-Feynman forces on each atom is less than 0.03 eV/Å in magnitude.

3 Results and Discussions

3.1 Structure and Stability of 2D-ZnO

Monolayer form of ZnO has a honeycomb lattice structure similar to BN [Fig. 1a]. Our estimate of its lattice constant, a = 3.30 Å is in good agreement with Topsakal *et al* (a_{GGA}=3.28Å).[38] The 2D-ZnO is sp^2 hybridized with a Zn-O bond length of 1.89 Å, 5% less than the 3D equivalent (2 Å) of ZnO with sp^3 hybridization.[38] To bench mark our results, we have estimated the cohesive energy, and analyzed the electronic structure and vibrational spectra of 2D-ZnO, and compared with the available results of Topsakal and coworkers, where they have used GGA approximated exchange correlation energy functional of Perdew-Wang 91 (PW91) parameterized form.[38] Cohesive energy(E_{coh}) of ZnO monolayer is determined using,

$$E_{coh} = E_T(2D-ZnO) - E_a^{isolated}(Zn) - E_a^{isolated}(O) \quad (1)$$

where, E_T is the total energy of the system and $E_a^{isolated}$ is the total energy of an isolated atom. Our estimate of E_{coh} is 8.29 eV per formula unit, in good agreement with Topsakal *et al* (8.42 eV).[38] Electronic structure of 2D-ZnO [Fig. 1b] shows that it is a direct band gap semiconductor with a gap of 1.62 eV. Taking into account the fact that band gaps are usually underestimated in DFT calculations, we expect 2D-ZnO to be

[a] *Address, Theoretical Sciences Unit, Jawaharlal Nehru Centre for Advanced Scientific Research, Jakkur, Bangalore 560 064, India*
[b] *Address, Sheik Saqr Laboratory, Jawaharlal Nehru Centre for Advanced Scientific Research, Jakkur, Bangalore 560 064, India*
[c] *Address, Physics Department, UAE University, P.O. Box 17551, Al-Ain, United Arab Emirates*
∗ Email: ntit@uaeu.ac.ae; ‡ Email: waghmare@jncasr.ac.in

rather a good insulator. We project out the density of states on individual atoms and orbitals to study the character of valence and conduction bands [Fig. 1b]. Energy band immediately below the gap, the valence band (-4 to -1.5 eV) is constituted primarily of p-orbital's of O and weakly of d-orbitals of Zn. Valence band deeper in energy (< -4 eV) arises from the d orbitals of Zn. Upper conduction bands are primarily constituted of the s orbitals of Zn.

Phonon spectrum, which is obtained as eigenvalues of the Hessian of total energy (dynamical matrix, second derivative of total energy with respect to atomic positions) reveal the structural stability of the system. Theoretical phonon dispersion of 2D-ZnO reveals that planar ZnO is locally stable [Fig. 1c], and weak instabilities of the ZA branch (out-of-plane acoustic mode) around the Γ point is an artifact of a finite mesh size.[38] Our results for phonon dispersion show similar behaviour as predicted by Topsakal *et al.*[38]

3.2 Configurations

We have considered four inequivalent configurations of 2D-ZnO-H_2S complex with different orientations of H_2S at various sites of the 2D-ZnO sheet: a) H_2S on the top of the center of the hexagonal ring, with the H atoms pointing away (configuration I), and towards (configuration II) the 2D-ZnO sheet, b) H_2S on top of the Zn-O bond with H and S lying in same plane parallel to 2D-ZnO sheet, H near O (configuration III) and away from O (configuration IV).

To quantify the strength of interaction between H_2S and 2D-ZnO, we obtain adsorption energy (E_A), as follows

$$E_A = \frac{E_{2D-ZnO-H_2S} - E_{2D-ZnO} - nE_{H_2S}}{n} \qquad (2)$$

where $E_{2D-ZnO-H_2S}$, E_{2D-ZnO}, E_{H_2S} are the total energies of the optimized structures of 2D-ZnO-H_2S complex, 2D-ZnO, isolated free H_2S molecule respectively, and n is the total number of H_2S molecules. Our results clearly reveal that, $E_A<0$ with magnitudes from -30 to -17 kJ mol^{-1}[Table 1] revealing a relatively weak adsorption of H_2S on 2D-ZnO. These values are intermediate to those of physisorption and chemisorption. Among these configurations, the configuration II with E_A = -29.7 kJ mol^{-1} is energetically more stable with the H_2S adsorbed at the center of ring and the H atoms oriented towards the 2D-ZnO sheet [Fig. 2b].

To identify the mechanism of adsorption at the atomistic level, we now consider the most stable configuration (configuration II). We find that only a few Zn-O bonds length in the vicinity of the adsorbed H_2S molecule change slightly, indicating a weak interaction between 2D-ZnO and H_2S. Zn-O bonds elongates by 0.8%, and there is slight bending (3.2°) in the 2D-ZnO sheet, while the H-S bond elongates by 1%. The distance between H_2S molecule and 2D-ZnO (O-H distance is 2.2 Å) is longer than a typical O-H bond length. To understand the nature of the interaction, we visualize the charge density plot of 2D-ZnO-H_2S complex [Fig. 2b]. Charge density isosurface shows a weak electrostatic interaction between H_2S molecule and the substrate.

We estimate the van der Waals contribution (E_A^v):

$$E_{A^v} = \frac{E_{2D-ZnO-H_2S^v} - E_{2D-ZnO^v} - nE_{H_2S^v}}{n}, \qquad (3)$$

where E_{x^v}, with x = 2D-ZnO-H_2S, 2D-ZnO, H_2S is the respective energy contribution due to dispersion correction. The vdW contribution(E_{A^v}) of configuration II is -24.4 kJmol^{-1} (where E_A= -29.7 kJmol$^-$1), showing that most of the binding during adsorption arises from vdW interactions.

3.3 Dependence of Adsorption on H_2S Coverage

The change in adsorption energy as a function of coverage of H_2S (for coverages of 26$-$230 mg of H_2S per g of 2D-ZnO) shows the same relative stability of four configurations, hence we will focus on the most stable configuration II. The amount of H_2S was varied while keeping the size of 2D-ZnO supercell (4 x 4 x 1) the same. We find that adsorption energy increases with concentration of H_2S, and saturates at coverages greater than 200 mg of H_2S per g of 2D-ZnO [Fig. 3a]. The adsorption energy increases with concentration due to a) an increase in the intramolecular interaction (E_{A^v}(HS)) between the condensed H_2S molecules, (E_{A^v}(HS) is calculated by freezing the H_2S molecules after isolating it from the complex), b) nearest distance between the H_2S molecules and 2D-ZnO sheet decreases (from 2.2 to 1.7 Å), which is less than the sum of the van der Waal radii of O (1.5 Å) and H (1 Å), resulting in electrostatic interaction. The vdW contribution to the overall adsorption energy decreases, as the repulsive term in the potential energy becomes dominant at shorter distance between H_2S molecules and 2D-ZnO sheet, which becomes further less than the sum of van der Waal radii with coverage of H_2S [Fig. 3a]. At higher coverages, buckling in 2D-ZnO is also significant, at the places where cations and anions (O and H, Zn and S) come close to each other. Here, visualization of charge density shows a relatively large overlap between densities of H_2S molecules and of the substrate indicating relevance of electrostatic interaction [see Inset Fig. 3b for coverage of 130 mg of H_2S per g of 2D-ZnO].

We now examine the electronic structure (DOS) of 2D-ZnO with and without absorbed H_2S molecules. The Fermi level is set to 0 is all the three cases [see Fig. 3b] with the coverage of 130 mg of H_2S per g of 2D-ZnO]. Comparing the DOS of 2D-ZnO, frozen/condensed H_2S molecule and the complex, we see a weak overlap of wavefunctions of H_2S with 2D-ZnO, and a slight increase in band gap by $\sim$0.2 eV indicating a weak covalent interaction of 2D-ZnO with H_2S molecules, primar-

ily associated with the interaction of p-orbitals of O with s-orbitals of H and s-orbitals of Zn with p-orbitals of S.

To understand further the adsorption, we have determined the charges using Löwdin method as implemented in Quantum Espresso and estimated the charge transfer:

$$QT = Q^{H_2S}_{2D-ZnO-H_2S} - Q^{H_2S}_{frozen} \quad (4)$$

where QT is the charge transfer, $Q^{H_2S}_{2D-ZnO-H_2S}$, $Q^{H_2S}_{frozen}$ is the sum of total charge on the atoms in frozen H_2S molecules, positive value indicates transfer of electron from substrate to molecule(s).

From the amount of charge transfer as a function of the coverage of H_2S [Fig 3c], it is clear that the total charge(e) transfer from the substrate to molecule increases with concentration, while the charge transfer per molecule (QT/n) decreases till $n = 6$ (156 mg of H_2S per g of 2D-ZnO), and increases with further increase in coverage. The total charge transfer varies from 0.1 to 0.25 electron, for the coverages studied here, responsible for a weak electrostatic interaction between the H_2S and 2D-ZnO substrate. Thus the adsorption of H_2S on 2D-ZnO is intermediate to physisorption and chemisorption with mixed vdW, electrostatic and weak covalent interactions.

3.4 Defects in 2D-ZnO and Their Effects on Adsorption

3.4.1 Stone-Wales defects. Stone-Wales(SW) defects are topological defects observed in two dimensional systems such as graphene and its sp^2 analogues.[39] We have explored the possibility of the existence of SW defects in 2D-ZnO obtained by in-plane rotation of one of the Zn-O bonds by 90°. On structural relaxation, we see that the Zn-O bond comes back to its original unrotated position, indicating that a SW defect is unstable. Stone-wales defects in other heteronuclear graphene analogues such as BN are known to be a meta-stable state due to high formation energy of homonuclear bonds between B-B and N-N, but the formation of Zn-Zn bond is very unlikely due to higher oxidation state and ionic size.[40,41] We also considered the case in which one of the Zn-O bond is rotated out-of plane by 90°, and see that on relaxation the out-of-plane Zn-O comes back to the original position, indicating that bond rotation does not lead to any metastable point defect formation.

3.4.2 N-substitution on oxygen site. We determined the effects of nitrogen substitution in 2D-ZnO, by replacing oxygen atoms with nitrogen. We considered N-substituted 2D-ZnO by replacing one of the oxygen atom with nitrogen atom initially in a 4x4 supercell of 2D-ZnO. Structural relaxation and phonon reveal a weak instability leading to out-of-plane displacements ($\sim$ 0.03 to 0.05 Å) of the adjacent Zn and O atoms with a moderate energy cost of 1.14 eV per N atom. Electronic band structure reveals presence of bands at Fermi level associated with p-orbital of nitrogen, similar to the isolated band corresponding to p-orbital of nitrogen in bulk ZnO resulting from substitutional doping with n-type elements (N and F) reported by Saha *et al*,[18] [see Fig 4a for electronic band structure of 2D-$ZnO_{1-x}N_y$ (black curve) with doping concentration 11%].

We have placed a H_2S molecule at a distance of 1 Å from the N-site with H facing towards the sheet, and relaxed the structure. We find a rather strong interaction of H_2S molecule and doped 2D-ZnO, with H_2S molecule dissociating to H^+ and HS^-. The doped 2D-ZnO sheet undergoes a local structural distortion involving bending by 5° and elongation of few Zn-O bonds ($\sim$4%) near H_2S. The charge density shows a strong overlap of densities of N of doped 2D-ZnO and isolated H^+ of H_2S forming a strong covalent bond (d_{H-N}=1.03 Å), whereas HS^- weakly interacts with Zn (d_{Zn-HS}=2.46 Å) [see Fig 4b]. The adsorption energy increases drastically to -152 kJ mol^{-1}. On comparing, the projected density of states of the complex with the substrate (not shown here), we observe that the increase in the adsorption is mainly due to overlap of s-orbital of H^+ with p-orbitals of N and there is a slight increase in the distance between HOMO and LUMO levels, with vanishing density of states at the Fermi level in the complex.

We now study the effect of concentration of substitutional nitrogen doping on the adsorption. We have considered a 3x3x1 supercell of ZnO with doping concentration varying from 5.5 to 22.2 atomic percent. Freezing of unstable modes to distort this structure leads to bending in 2D-$ZnO_{1-x}N_y$ sheet with out-of-plane displacement ($\sim$ 0.2 to 0.3 Å) of adjacent atoms with reasonable formation energy ($\sim$0.9 eV to 1.1 eV/N atom). We have placed the H_2S molecule at a distance of 1 Å above one of the nitrogen atoms with hydrogen atoms closer to the sheet. The adsorption energy increases till 11% doping concentration and saturates for higher doping concentration for a coverage of 46.8 mg of H_2S per g of 2D-$ZnO_{1-x}N_y$ [see Fig 4c]. As the concentration of nitrogen increases, the charge transfer from the molecule to substrate increases and distance between dissociated H_2S molecule and substrate decreases as the substrate becomes more electronegative [see Inset Fig 4c]. The position and orientation of H_2S molecule is very important, as the strength of adsorption decreases drastically when placed away from the vicinity of defect site.

For a fixed doping concentration (11%), we vary the concentration of the H_2S from 46.8 to 234 mg of H_2S per g of 2D-$ZnO_{1-x}N_y$. As the coverage of H_2S increases, the adsorption energy per molecule decreases [see Fig 4d]. An increased electrostatic interaction between H_2S molecules and the substrate is evident from structural distortion of the relaxed structure. It is clear in the electronic structure for a coverage of 93.6 mg of H_2S [see Fig 4a], the sub bands at the Fermi level corresponding to p-orbitals of nitrogen shift down in energy

opening a gap, and the gap increases with the coverage of H_2S, due to formation of strong covalent bond with H leading to splitting of H_2S. The decrease in adsorption energy can be attributed to a) saturation of nitrogen dangling bonds, b) decrease in the average distance between the H_2S molecules and substrate and c) decrease in the total charge transfer with concentration, though charge transfer per molecule is same.

3.4.3 Oxygen vacancy. We now determine how oxygen vacancies in 2D-ZnO influence the adsorption of H_2S. Removing one of the oxygen atom from the pristine 4x4 supercell of 2D-ZnO, i.e, creating a vacancy of 3.15 atomic percent, We first optimized the structure. Our estimate of the formation energy of oxygen vacancy is a bit high (8.05 eV/vacancy). We initially placed H_2S molecules at a distance of 1Å from the O-vacancy with H and S in same plane parallel to the sheet. We find that the presence of oxygen vacancy leads to negligible increase in the adsorption energy ($\sim$ 1 kJ/mol) of H_2S.

We now increase the coverage of H_2S and place H_2S molecules in the vicinity of an oxygen vacancy. At lower coverages of H_2S ($\leq$52 mg of H_2S per g of 2D-ZnO_{1-x}), there is negligible effect on the strength of adsorption. As the coverage of H_2S increases adsorption energy increases due to increase in electrostatic interaction among the H_2S molecules and substrate, this is evident in structural distortions that lead to splitting of H_2S accompanied by formation of H_2 molecule [see Fig 5a]. The primary reason for the splitting of H_2S is that O-vacancy site is replaced by S of H_2S indicating essential role of O-vacancy in H_2 production [see Inset Fig 5a]. The above reaction can be written as

$$2D-ZnO_{1-x}+2H_2S \rightarrow H_2+HS\text{–}(2D-ZnO_{1-x})||||HS, \quad (5)$$

To calculate the amount of energy required to separate the H_2 from the complex, we have displaced the H_2 away from substrate. The amount of energy required to separate the H_2 molecule from the complex is quite low ($\sim$0.07 eV/molecule), indicating that 2D-ZnO_{1-x} may be a good candidate for the production of hydrogen fuel [see Fig 5b, where d_o is the distance between the substrate and H_2 molecule in the relaxed structure, d is the distance of H_2 from the equilibrium position in the relaxed structure and E_o, E_d is the corresponding energy]. To explore the disproportionation of two HS radicals present at the adjacent adsorption sites, given by

$$HS^* + HS^* \rightarrow H_2S + S^*, \quad (6)$$

we have decreased the distance between two HS radicals and relaxed the structure. We see a strong repulsion between HS radicals leading to no disproportionation at low concentration of vacancy and coverage of H_2S.

To explore the reusability of defected material, we calculate the energy required to regenerate 2D-ZnO_{1-x} (E_R) from the sulphonated 2D-ZnO_{1-x}. E_R is determined using,

$$E_R = E_{2D-ZnO_{1-x}} - [E_{2D-ZnO_{1-x}S_x} - E_a^{isolated}(S)] \quad (7)$$

where, $E_{2D-ZnO_{1-x}}$, $E_{2D-ZnO_{1-x}S_x}$ and $E_a^{isolated}(S)$ are the total energies of 2D-ZnO_{1-x}, sulphonated 2D-ZnO_{1-x} and isolated sulphur atom respectively. Our estimate of energy cost of regenerating 2D-ZnO_{1-x} with 3.15 atomic percent sulphonated 2D-ZnO_{1-x} is 4.15 eV/S atom, which is less compared to formation energy of 3.15 atomic percent oxygen vacancy in prisitine 2D-ZnO (8.05 eV/vacancy), indicating that regeneration of 2D-ZnO_{1-x} from 2D-$ZnO_{1-x}S_x$ is easier compared to introducing oxygen vacancy.

3.4.4 Selectivity of adsorbate molecules on 2D-ZnO_{1-x}/2D-$ZnO_{1-x}N_y$. To check the selectivity of H_2S over other potentially reactive species like CO_2 and H_2O on defected 2D-ZnO, we have intially placed single gas molecule of CO_2/H_2O in the vicinity of oxygen vacancy at a distance of 1 Å from the substrate (2D-ZnO_{1-x}, 3.15 atomic percent oxygen vacancy). For the low concentrations of CO_2 considered (34 mg of CO_2 per g of 2D-ZnO_{1-x}), the E_A is positive (30 kJ/mol) indicating no adsorption, where as H_2O bonds relatively stronger than H_2S, since O is more electronegative than sulphur. In neither of the cases (CO_2 or H_2O), the adsorbed gas molecule dissociates and fills the oxygen vacancy. We have also studied selectivity of H_2O over H_2S in presence of N-doping (3.15 atomic percent N-doping), We find that H_2O unlike H_2S does not dissociate to saturate the dangling bonds of N, instead bonds weakly with 2D-$ZnO_{1-x}N_y$ [see energetics in Table 2]. H_2S binds preferrentially over CO_2/H_2O

4 Conclusion

We find that the adsorption of H_2S on pristine 2D-ZnO is weak and mainly due to the van der Waals interaction for lower coverage of H_2S, and H_2S molecule prefers to occupy the site at center of hexagonal ring with the H atoms pointing towards the oxygen atoms of the substrate. N-substitution at O-sites leads to a marked increase in adsorption energy (by $\sim$5 times) with respect to the pristine 2D-ZnO, resulting in dissociation of H_2S. The adsorption energy increases with doping concentration and saturates above 11% defect concentration for a coverage of 46.8 mg of H_2S per g of 2D-$ZnO_{1-x}N_y$. When the coverage of H_2S increases for a fixed N-doping concentration, we see that the adsorption energy per molecule decreases due to saturation of N-dangling bonds, the decrease in the total charge transfer as well as increase in the average distance between all the H_2S molecules and the substrate. O-vacancy has little effect on the adsorption at lower coverages of H_2S, but it strengthens with increase in the coverage due to electrostatic interactions. This leads to splitting of H_2S molecules in which

S relocates to the site of O-vacancy in 2D-ZnO_{1-x} and H_2 is released. We find that the SW defects are unstable in 2D-ZnO.

Thus, we find that both N-substitution and Oxygen vacancies in 2D-ZnO facilitate capture of H_2S and its splitting to generate H_2. The former has applications in maintaining clean environment and the latter is useful as a green fuel for energy. In fact, the end product after consumption of this fuel is water which also enriches the quality of environment.

Acknowledgements

The authors are indebted to Profs. C.N.R. Rao, Z.H. Yamani and N. Tabet for many fruitful discussions. S.K. is grateful for TUE-CMS, JNCASR for computational facility and a research fellowship from the Council of Scientific and Industrial Research, India. U.V.W. acknowledges funding from Nano Mission, Department of Science and Technology, India. N.T is thankful to Profs. C.N.R. Rao and Z.H. Yamani for supporting his visit to JNCASR.

References

1 J. Lindenmann, V. Matzi, N. Neuboeck, B. Ratzenhofer-Komenda, A. Maier, F.-M. Smolle-Juettner *et al.*, *Diving and hyperbaric medicine: the journal of the South Pacific Underwater Medicine Society*, 2010, **40**, 213–217.

2 E. R. Parivash Dezham and D. Jenkins, *International Journal of Quantum Chemistry*, 1988, **60**, 514–517.

3 Q.-L. Tang, *International Journal of Quantum Chemistry*, 2013, **113**, 1992–2001.

4 J. A. Rodriguez, T. Jirsak, M. Prez, S. Chaturvedi, M. Kuhn, L. Gonzlez and A. Maiti, *Journal of the American Chemical Society*, 2000, **122**, 12362–12370.

5 B. G. et al, *Energy Progress*, 1986, **6**, 71–75.

6 J. Zaman and A. Chakma, *Fuel Processing Technology*, 1995, **41**, 159 – 198.

7 O. Schmidt, A. Geis, P. Kiesel, C. G. V. de Walle, N. M. Johnson, A. Bakin, A. Waag and G. H. Dhler, *Superlattices and Microstructures*, 2006, **39**, 8 – 16.

8 O. Schmidt, P. Kiesel, C. G. V. de Walle, N. M. Johnson, J. Nause and G. H. Döhler, *Japanese Journal of Applied Physics*, 2005, **44**, 7271–7274.

9 G. F. Fine, L. M. Cavanagh, A. Afonja and R. Binions, *Sensors*, 2010, **10**, 5469–5502.

10 M. Hulko, I. Hospach, N. Krasteva and G. Nelles, *Sensors*, 2011, **11**, 5968–5980.

11 E. Comini, G. Faglia, G. Sberveglieri, Z. Pan and Z. L. Wang, *Applied Physics Letters*, 2002, **81**, 1869–1871.

12 C. Li, D. Zhang, X. Liu, S. Han, T. Tang, J. Han and C. Zhou, *Applied Physics Letters*, 2003, **82**, 1613–1615.

13 X. Zou, J. Wang, X. Liu, C. Wang, Y. Jiang, Y. Wang, X. Xiao, J. C. Ho, J. Li, C. Jiang, Y. Fang, W. Liu and L. Liao, *Nano Letters*, 2013, **13**, 3287–3292.

14 D. N. Huyen, N. T. Tung, N. D. Thien and L. H. Thanh, *Sensors*, 2011, **11**, 1924–1931.

15 K. K. Kasem, *Journal of Materials Sciences and Technology*, 2010, **26**, 619.

16 O. Bikondoa, C. L. Pang, R. Ithnin, C. A. Muryn, H. Onishi and G. Thornton, *Nature Materials*, 2006, **5**, 189–192.

17 J. A. Rodriguez, S. Chaturvedi, M. Kuhn and J. Hrbek, *The Journal of Physical Chemistry B*, 1998, **102**, 5511–5519.

18 R. Saha, S. Revoju, V. I. Hegde, U. V. Waghmare, A. Sundaresan and C. N. R. Rao, *ChemPhysChem*, 2013, **14**, 2672–2677.

19 D. Thomas, *Journal of Physics and Chemistry of Solids*, 1960, **15**, 86–96.

20 D. Reynolds, D. Look and B. Jogai, *Solid State Communications*, 1996, **99**, 873 – 875.

21 D. C. Reynolds, D. C. Look, B. Jogai, C. W. Litton, G. Cantwell and W. C. Harsch, *Phys. Rev. B*, 1999, **60**, 2340–2344.

22 Y. Chen, D. M. Bagnall, H.-j. Koh, K.-t. Park, K. Hiraga, Z. Zhu and T. Yao, *Journal of Applied Physics*, 1998, **84**, 3912–3918.

23 A. Ohtomo, M. Kawasaki, T. Koida, K. Masubuchi, H. Koinuma, Y. Sakurai, Y. Yoshida, T. Yasuda and Y. Segawa, *Applied Physics Letters*, 1998, **72**, 2466–2468.

24 A. Ohtomo, R. Shiroki, I. Ohkubo, H. Koinuma and M. Kawasaki, *Applied Physics Letters*, 1999, **75**, 4088–4090.

25 T. Makino, C. H. Chia, N. T. Tuan, Y. Segawa, M. Kawasaki, A. Ohtomo, K. Tamura and H. Koinuma, *Applied Physics Letters*, 2000, **77**, 1632–1634.

26 Z. Tu, *Journal of Computational and Theoretical Nanoscience*, 2010, **7**, 1182–1186.

27 M.-W. Ahn, K.-S. Park, J.-H. Heo, J.-G. Park, D.-W. Kim, K. J. Choi, J.-H. Lee and S.-H. Hong, *Applied Physics Letters*, 2008, **93**, –.

28 Y.-H. Zhang, L.-F. Han, Y.-H. Xiao, D.-Z. Jia, Z.-H. Guo and F. Li, *Computational Materials Science*, 2013, **69**, 222–228.

29 S. C. Lee, S. Y. Kim, B. W. Hwang, S. Y. Jung, D. Ragupathy, I. S. Son, D. D. Lee and J. C. Kim, *Sensors*, 2013, **13**, 3889–3901.

30 V. I. Hegde, S. N. Shirodkar, N. Tit, U. V. Waghmare and Z. H. Yamani, *Surface Science*, 2014, **621**, 168 – 174.

31 P. Giannozzi, S. Baroni, N. Bonini, M. Calandra, R. Car, C. Cavazzoni, D. Ceresoli, G. L. Chiarotti, M. Cococcioni, I. Dabo, A. Dal Corso, S. de Gironcoli, S. Fabris, G. Fratesi, R. Gebauer, U. Gerstmann, C. Gougous-

sis, A. Kokalj, M. Lazzeri, L. Martin-Samos, N. Marzari, F. Mauri, R. Mazzarello, S. Paolini, A. Pasquarello, L. Paulatto, C. Sbraccia, S. Scandolo, G. Sclauzero, A. P. Seitsonen, A. Smogunov, P. Umari and R. M. Wentzcovitch, *Journal of Physics: Condensed Matter*, 2009, **21**, 395502 (19pp).

32 J. P. Perdew, K. Burke and M. Ernzerhof, *Phys. Rev. Lett.*, 1996, **77**, 3865–3868.

33 S. Grimme, *Journal of Computational Chemistry*, 2006, **27**, 1787–1799.

34 D. C. Langreth and M. J. Mehl, *Phys. Rev. B*, 1983, **28**, 1809–1834.

35 J. P. Perdew, *Phys. Rev. Lett.*, 1985, **55**, 1665–1668.

36 J. P. Perdew and W. Yue, *Phys. Rev. B*, 1986, **33**, 8800–8802.

37 D. Vanderbilt, *Phys. Rev. B*, 1990, **41**, 7892–7895.

38 M. Topsakal, S. Cahangirov, E. Bekaroglu and S. Ciraci, *Phys. Rev. B*, 2009, **80**, 235119.

39 J. C. Meyer, C. Kisielowski, R. Erni, M. D. Rossell, M. Crommie and A. Zettl, *Nano letters*, 2008, **8**, 3582–3586.

40 F. A. Cotton, *Accounts of Chemical Research*, 1969, **2**, 240–247.

41 J. Sheldon, *Australian Journal of Chemistry*, 1964, **17**, 1191–1196.

5 Tables and Graphics

5.1 Tables

Table 1 Energy of Adsorption, E_A (kJ mol^{-1}) with nearest distances between the substrate and molecule for various configurations

		Nearest distance	
Configuration	E_A	d_{Zn-S} (Å)	d_{O-H} (Å)
I	−17.2	3.2	3.96
II	−29.7	3.51	2.22
III	−24.3	2.77	3.05
IV	−14.6	3.61	3.88

Table 2 Comparison of energetics for selectivity of H_2S over CO_2 and H_2O

Substrate	Molecule	E_A (kJmol^{-1})
2D-ZnO_{1-x}	H_2S	−28.9
	CO_2	30.3
	H_2O	−43.2
2D-$ZnO_{1-x}N_y$	H_2S	−151.0
	H_2O	−35.4

5.2 Graphics

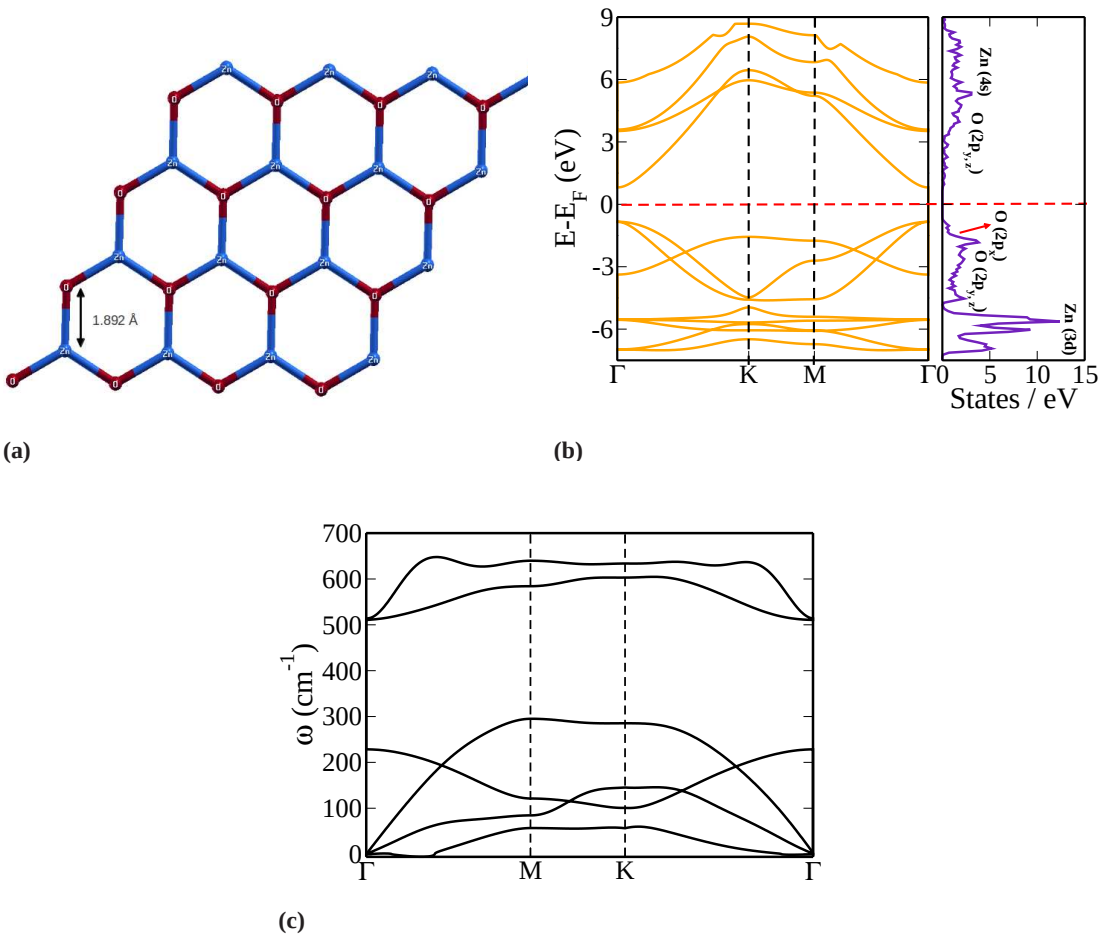

(a) (b) (c)

Fig. 1 (a) Relaxed structure,(b) electronic structure and (c) phonon dispersion of 2D monolayer ZnO

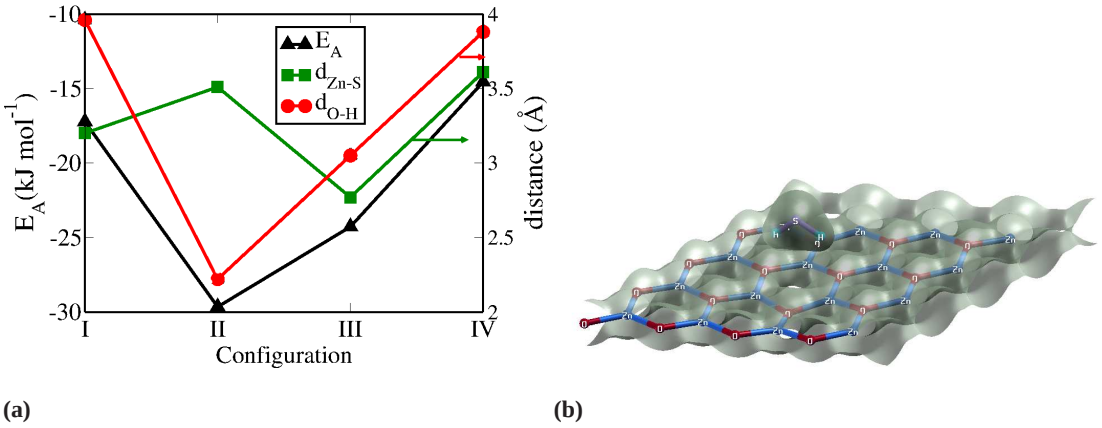

(a) (b)

Fig. 2 (a) Adsorption energy, nearest distances between the H_2S molecule and 2D-ZnO sheet for different configurations, (b) charge density plot for the coverage of 130.89 mg of H_2S per g of 2D-ZnO

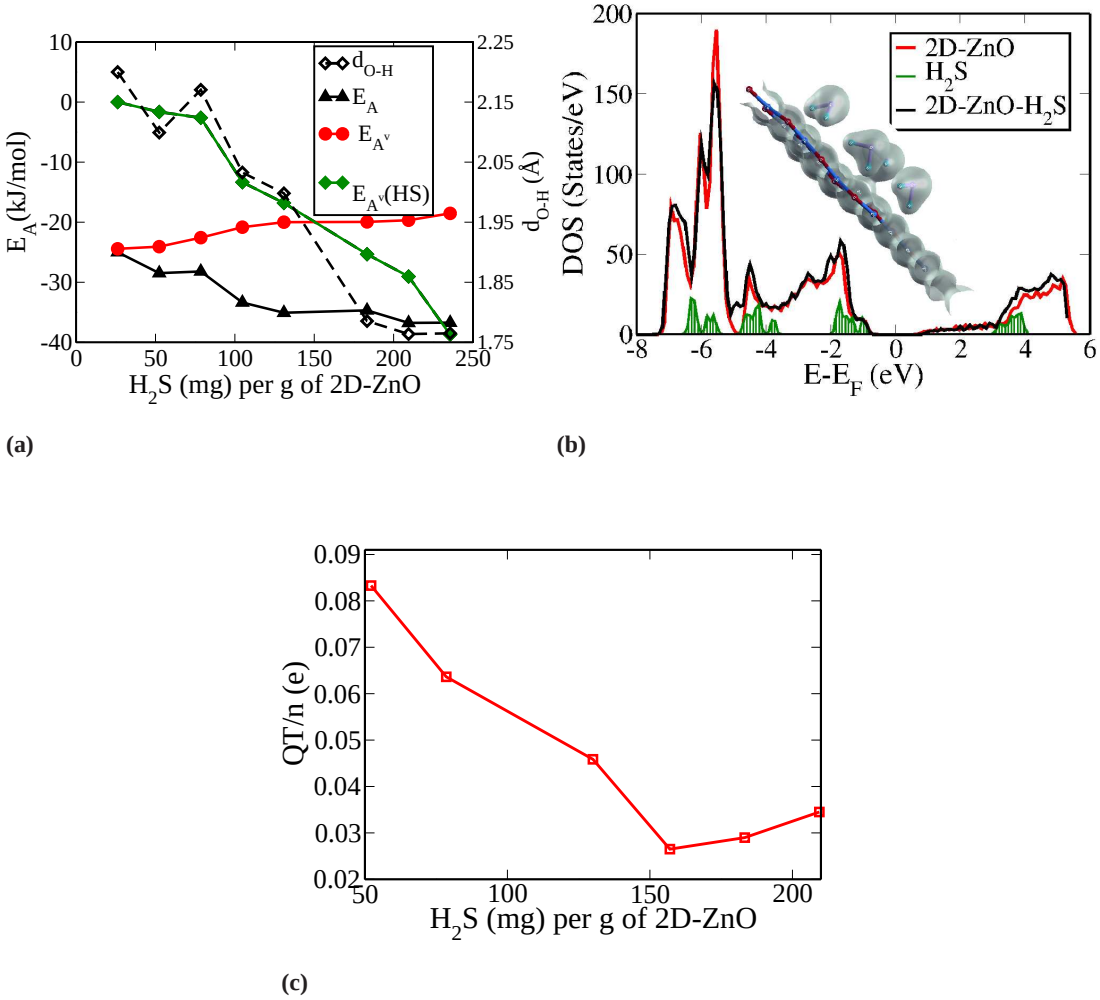

Fig. 3 (a) Energy of adsorption, vdW contribution to total adsorption of H_2S on 2D-ZnO sheet as a function of coverage with the smallest distance between H_2S and 2D-ZnO sheet, (b) comparison of electronic density of states of the complex with the coverage 130 mg of H_2S per g of 2D-ZnO with the pristine 2D-ZnO, inset shows charge density plot of the complex, and (c) total charge transfer per molecule from substrate to molecules with respect to coverage

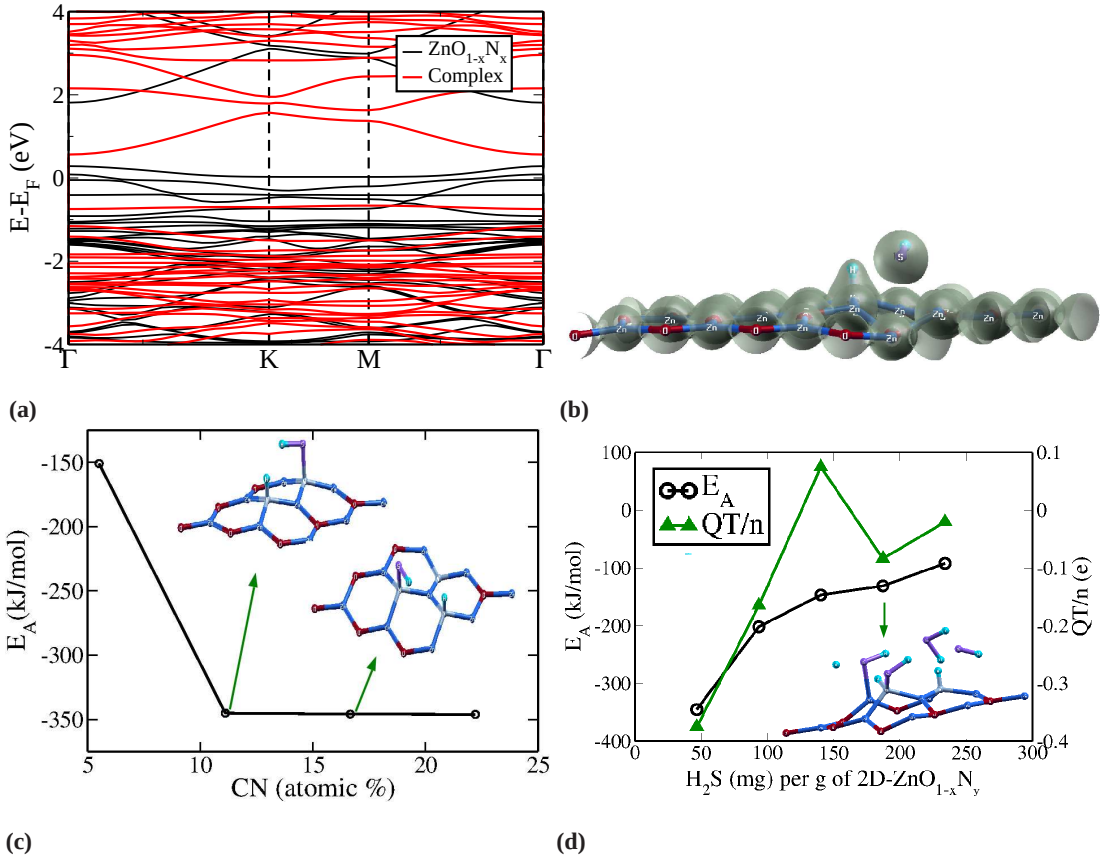

Fig. 4 (a) Comparison of electronic band structure of 2D-$ZnO_{1-x}N_y$ and its complex with coverage of 93.6 mg of H_2S per g of 2D-$ZnO_{1-x}N_y$, (b) charge density plot of a complex with doping concentration(CN) 3.1% and H_2S coverage 26 mg per g of 2D-$ZnO_{1-x}N_y$, (c) adsorption energy as a function of doping concentration for a coverage of 46.8 mg of H_2S per g of 2D-$ZnO_{1-x}N_y$. The inset figures corresponds to doping concentration 11% (left) and 16.7% (right), and (d) adsorption energy as a function of H_2S coverage for a fixed doping concentration (11.1% N), the inset figure corresponds to H_2S coverage of 189.2 mg per g of 2D-$ZnO_{1-x}N_y$

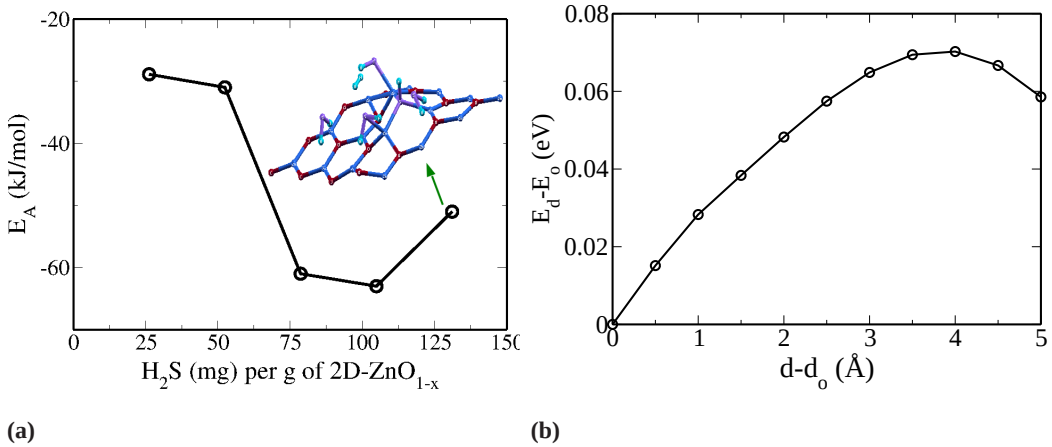

Fig. 5 (a) Adsorption energy as a function of H_2S coverage for a fixed oxygen vacancy, the inset figure corresponds to coverage of 130 mg of H_2S per g of 2D-ZnO_{1-x}, and (b) difference in energy of system with H_2 displaced at distance of d (Å) away from the equilibrium distance (d_o) in the relaxed structure for a coverage of 130 mg of H_2S per g of 2D-ZnO_{1-x}

Table of Contents

We report novel applications of inorganic analogue of graphene (2D-ZnO) in the detection and capture of toxic H_2S gas and conversion to a green fuel, hydrogen using first-principles density functional theory calculations. Presence of O-vacancy in the 2D-ZnO facilitates dissociation of H_2S into H_2 and sulphur filling the site of O-vacancy. Presence of dangling bonds of N in N-doped 2D-ZnO is also shown to bind strongly with H_2S, and facilitate its dissociation and elimination from environment.